Energy, Mines and Resources Canada | Énergie, Mines et Ressources Canada

CANMET

Canada Centre for Mineral and Energy Technology | Centre canadien de la technologie des minéraux et de l'énergie

THE EFFECTS OF LESS COMMONLY ENCOUNTERED IMPURITIES ON ZINC ELECTROWINNING FROM INDUSTRIAL ACID SULPHATE ELECTROLYTE

D.J. MacKinnon, J.M. Brannen and P.L. Fenn
Metallurgical Chemistry Section
Extractive Metallurgy Laboratory

October 1985

Project: MRP-3.0.77.01
Silver Recovery in the Zinc Industry

This document is an unedited ... (CANMET)

Ce document est un rapport ... (CANMET)

43pp

MINERALS RESEARCH PROGRAM
MINERAL SCIENCES LABORATORIES
DIVISION REPORT MRP/MSL 85-144 (TR)

Crown Copyrights Reserved

MICROMEDIA

MAR 3 1986

THE EFFECTS OF LESS COMMONLY ENCOUNTERED IMPURITIES ON ZINC ELECTROWINNING FROM INDUSTRIAL ACID SULPHATE ELECTROLYTE

by

D.J. MacKinnon*, J.M. Brannen** and P.L. Fenn***

ABSTRACT

The effects of As(III), As(V), Bi, Ga, In, Se, Te and Tl and their interaction with glue on the current efficiency (CE) and polarization behaviour of zinc deposition and on the morphology and preferred orientation of 1-h Zn deposits electrowon from industrial acid sulphate electrolyte have been determined. Trivalent arsenic and indium had no effect on the CE and did not alter significantly the zinc deposition polarization curve. They also did not alter the Zn deposit morphology or its preferred orientation. Thallium increased both the CE for zinc deposition and the zinc deposition polarization. It also produced a significant change in both the Zn deposit morphology and orientation.

Increasing concentrations of As(V), Bi and Ga in the electrolyte resulted in a linear decrease in the CE for zinc deposition; the detrimental

---

* Research Scientist, ** Research Technician and *** COSEP Student, Metallurgical Chemistry Section, Mineral Sciences Laboratories, CANMET, Energy, Mines and Resources Canada, 555 Booth Street, Ottawa, Ontario K1A 0G1.

effect on the CE increased in the order: Ga<Bi<As(V). These impurities also depolarized the zinc deposition reaction and produced characteristic changes during the reverse scan of the cyclic voltammograms. However, these impurities had dissimilar effects on the Zn deposit morphology and orientation.

Selenium and tellurium caused a very rapid decrease in the zinc deposition CE and had similar, characteristic effects on zinc deposition polarization curves. Both these impurities produced changes in the Zn deposit morphology and orientation.

The addition of glue in combination with the above mentioned impurities was generally not effective in counteracting their detrimental effects on zinc electrowinning.

LES EFFETS DES IMPURETÉS RENCONTRÉES MOINS FRÉQUEMMENT LORS DE L'EXTRACTION ÉLECTROLYTIQUE DU ZINC À PARTIR D'UNE SOLUTION INDUSTRIELLE DE SULFATE ACIDE

par

D.J. MacKinnon*, J.M. Brannen** et P.L. Fenn***

RÉSUMÉ

On a déterminé les effets de As (III), As (V), Bi, Ga, In, Se, Te, et Tl ainsi que leur interaction avec de la colle sur le rendement électrique et le comportement de la polarisation du processus de dépôt du zinc et sur la morphologie et l'orientation préférée de ces dépôts de Zn obtenus en 1 heure à partir d'une solution industrielle de sulfate acide. L'arsenic trivalent et l'indium n'ont eu aucun effet sur le rendement électrique et n'ont pas changé la courbe de polarisation du processus de dépôt du zinc de façon significative. De plus, ils n'ont pas changé la morphologie du dépôt de zinc ou même l'orientation préférée de ce dépôt. Le thallium a augmenté le rendement électrique des dépôts du zinc ainsi que la polarisation du processus de dépôt du zinc. Il a aussi produit un changement significatif de la morphologie et de l'orientation du dépôt de zinc.

Une augmentation des concentrations de As (V), Bi et Ga dans la solution a produit une diminution linéaire du rendement électrique du processus de dépôt de zinc; l'effet nuisible sur le rendement électrique a augmenté dans l'ordre: Ga < Bi < As (V). Ces impuretés ont aussi dépolarisé la réaction du processus de dépôt du zinc et ont produit des

---

*Chercheur scientifique, **technicien chercheur et ***étudiant PEÉAC, Section de la chimie métallurgique, Laboratoires des sciences minérales, CANMET, Énergie, Mines et Ressources Canada, 555, rue Booth, Ottawa (Ontario) K1A 0G1.

changements caractéristiques au cours du balayage inverse des voltamogrammes cycliques. Ces impuretés avaient cependant des effets dissemblables sur la morphologie du processus de dépôt du zinc ainsi que sur l'orientation de ce dépôt.

Le sélénium et le tellure ont causé une baisse très rapide du rendement électrique du processus de dépôt du zinc et ont démontré des effets caractéristiques semblables sur les courbes de polarisation de ce dépôt. Ces deux impuretés ont produit des changements dans la morphologie et l'orientation du processus de dépôt du zinc.

On a constaté qu'en général l'addition de colle combinée aux impuretés susmentionnées n'était pas efficace pour contrebalancer leurs effets nuisibles sur l'extraction électrolytique du zinc.

—

1. INTRODUCTION

During the past several years reports have been published which characterized the effects of commonly encountered impurities on zinc electrowinning from acid sulphate electrolytes in terms of current efficiency, zinc deposition polarization, deposit morphology and orientation. Thus the effects of Sb (1-3), Co and Ni (4-10), Ge (6,7,11), Pb (12) and Cd (13,14) have been documented. Although these studies have provided a better understanding of impurity behaviour and have suggested the development of better control measures to counteract their deleterious effects, the mechanisms by which the impurities become activated in the electrolyte are still not fully understood.

Because these impurities are not usually present in purified zinc electrolyte to a significant degree, they have not been studied in detail. Weaver (15) reported that even small concentrations (<1 mg/L) of Se and Te are harmful to zinc electrowinning. Selenium, at 0.1 mg/L, produces a zinc deposit with heavy ridges. Higher concentrations raise spots on the face of the cathode with corresponding depressions on the reverse side. Excessive amounts (?) of Se cause severe re-solution of the zinc deposit. Tellurium is especially harmful in the presence of Co (15). Tellurium results in a rapid decrease in zinc deposition current efficiency (16); the presence of 1 mg/L Te prevents zinc deposition (17).

Kerby et al. (16), however, found that Se increased the current efficiency when present in the electrolyte in concentrations up to 20 mg/L. They interpreted this result in terms of the high hydrogen overvoltage on Se and to the poisoning of hydrogen evolution sites on the zinc deposit caused by the formation of selenium hydrides. Kerby et al. (16) speculated that the contradictory results obtained for Se might be caused by the presence of other impurities or by the ionic form in which Se exists in solution.

Kerby et al. (16) found that both In and Tl decreased the zinc deposition current efficiency whereas As(III) produced a slight increase in current efficiency. It has been reported (17) that Tl codeposits with Zn but has no appreciable effect on current efficiency.

In the present study, the effects of less commonly encountered impurities on the current efficiency and polarization behaviour of zinc deposition and on the morphology and orientation of l-h zinc deposits electrowon from industrial acid sulphate electrolyte were determined. It was felt that this information would add to the knowledge of impurity behaviour in general and might provide further insight into the mechanism of impurity interaction in the zinc electrowinning system. The impurities chosen for this study included As(III), As(V), Bi, Ga, In, Se, Te and Tl.

In the ensuing Results and Discussion Section, the data obtained for the various impurities are presented in groups according to where the impurity elements reside in the Periodic Table. Thus, the results are presented as Group IIIA (Ga, In, Tl), Group VA (As, Bi) and Group VIA (Se, Te).

2. EXPERIMENTAL PROCEDURE

2.1 Electrolyte and Apparatus

The electrolyte was an industrial zinc sulphate solution prepared from hot zinc dust purified neutral zinc electrolyte obtained from Cominco Ltd., Trail, British Columbia. The average analysis was in g/L: Zn 150, $MgSO_4$ 38, Mn 1.6; in mg/L: Cd 0.2, Sb 0.02, Co 0.3, Ge 0.01, Ni 0.1, Cu 0.1, Fe 0.9, Pb 0.2, Cl 80, F 3.

Cell solutions were prepared by adding H_2SO_4, redistilled water and impurities to the electrolyte to give final concentrations of 55 g/L Zn and 150 g/L H_2SO_4. Animal glue additions were made as concentrated solutions. The various impurities (In, Ga, Tl, As(III), As(V), Bi, Se and Te) were added as aliquots from their respective stock solutions.

The electrolysis cell consisted of a 1 L beaker fitted with a Lucite cover which had slots cut in it to mount the electrodes (3). A three electrode assemblage consisting of a central aluminum cathode and two platinum anodes was used. The cathode was fashioned from 4.7 mm thick Al sheet (purity 99.6%) obtained from Cominco. It measured 31.8 x 136.3 mm and was mounted so that zinc deposited on both sides onto a total area of 12.9 cm^2. The anodes were cut from a 0.3 mm thick Pt sheet and measured 17.9 x 109.7 mm. The platinum anodes were used to avoid Pb contamination on the zinc deposits from conventional Pb-Ag anodes (12).

2.2 Electrolysis

The electrolysis experiments were run in a constant temperature bath at 35°C with stirring, and at a cathode current density of 430 A/m^2 for a period of one hour.

2.3 Examination of Deposits

Sections of the zinc deposits were examined by scanning electron microscopy to determine the surface morphology of the deposit and by X-ray diffraction to determine the preferred crystal orientation relative to the ASTM standard for zinc powder. One side of the deposits electrowon from selected electrolytes was dissolved in HNO_3 for chemical analysis to determine the impurity content of the deposits by atomic absorption spectrophotometry.

2.4 Cyclic Voltammetry

Cyclic voltammograms were obtained using a voltage scan generator, a potentiostat and a x-y recorder for recording current versus applied potential plots. The voltage scan generator was used to cycle the potential from -0.95 V to about -1.15 V versus a saturated calomel electrode. The latter limit was determined to give a maximum current of approximately 65 mA on the forward scan; hence there is some variation in the potential scan range. The scan was done at a rate of 2 mV/s.

The same cell was used for both the cyclic voltammetry and the electrowinning; however, the electrode assembly differed. The working electrode was an aluminum cathode measuring 15.4 mm by 109.5 mm by 0.8 mm thick. It was mounted so that the surface area was approximately 3.2 cm^2. The counter electrode was one of the platinum anodes used in electrowinning. A saturated calomel electrode mounted adjacent to the cathode was used as the reference electrode.

Prior to each test the cathode was conditioned by polishing with 600 grit paper, washing with acetone followed by redistilled water, and patting dry with a tissue. The cathode was then put into the cell while the electrolyte was stirred. Once a steady rest potential was established, the stirrer was turned off and the scan was initiated.

3. RESULTS AND DISCUSSION

3.1 Current Efficiency

The effect of the Group IIIA impurities, (Ga, In and Tl) on the current efficiency (CE) for 1-h zinc deposits electrowon at 430 A/m^2 is shown in Figure 1. Both In and Tl have only a slight effect on the CE for concentrations up to 50 mg/L; the presence of Tl causes a small increase

whereas In results in a slight decrease in CE. The presence of Ga in the electrolyte produces a rapid linear decrease in CE.

The effect of increasing glue concentration on the CE for 1-h zinc deposits electrowon at 430 A/m^2 from electrolytes containing 20 mg/L of the Group IIIA impurities is shown in Figure 2. The presence of glue results in a significant decrease in the CE for electrolytes containing 20 mg/L In and Tl with the greater decrease occurring for the In-containing electrolyte (cf. Fig. 2). The addition of glue to 50 mg/L causes a slight overall decrease in the CE for an electrolyte containing 20 mg/L Ga.

The effect of the Group VA impurities, (As and Bi) on the CE for 1-h Zn deposits electrowon at 430 A/m^2 is shown in Figure 3; both the As(III) and As(V) forms were studied. As indicated in Figure 3, As (III) concentrations to 50 mg/L had no effect on the CE. The presence of even low concentrations of As(V), however, caused a dramatic decrease in the CE. The CE decreased linearly with increasing concentrations of As(V) to 20 mg/L; at concentrations >20 mg/L the decrease in CE was lower but the CE at 30 mg/L As(V) was only 20%.

Increasing Bi concentrations also resulted in a linear decrease in CE but the rate of decrease was intermediate between that of As(III) and As(V); the decrease in CE observed for increasing Bi concentration was similar to that observed for Ga, (cf. Fig. 1).

The addition of glue in the presence of Group VA impurities was not effective in counteracting the adverse effects of As(V) and Bi on the CE, Figure 4. It can be seen from Figure 4 that increasing glue concentration (in the absence of added impurity) results in a gradual decrease in CE; in the presence of 40 mg/L As(III), the decrease in CE with increasing glue concentration is further enhanced.

For an electrolyte containing 20 mg/L Bi, the addition of increasing glue concentration results in an initial decrease in CE; at higher glue concentrations, >10 mg/L, the CE increases but remains slightly below the 0 mg/L glue value. A somewhat similar trend is observed for As(V), but the overall effect is a decrease in CE.

The effect of the Group VIA impurities, (Se and Te) on the CE for 1-h Zn deposits electrowon at 430 A/m^2 is shown in Figure 5. The CE decreased rapidly with the addition of 1 mg/L Te or Se to the electrolyte; for concentrations of these impurities >1 mg/L the CE continued to decrease but at a much slower rate. The CE was virtually 0% when the concentration of these impurities reached 8 mg/L.

The addition of 10 mg/L glue to electrolytes containing 2 mg/L of Se and Te, respectively, resulted in a decrease in CE for the Se case but increased the CE in the case of Te, Figure 6.

3.2 Deposit Morphology and Orientation

The effect of the Group IIIA impurities (Ga, In and Tl) on the morphology of the 1-h zinc deposits electrowon at 430 A/m^2 in the presence and absence of glue is shown in a series of SEM photomicrographs, Figure 7. The effect of these impurities in the presence and absence of glue on the preferred orientation of selected deposits is summarized in Table 1.

Although the addition of Ga to the electrolyte resulted in a substantial decrease in CE, the morphology (Figure 7(a)) and preferred orientation (Table 1) of the 1-h Zn deposit remained unchanged from that obtained from addition-free electrolyte (3). The deposit morphology was characterized by well-defined hexagonal platelets aligned at intermediate angles to the Al cathode, resulting in a [112] preferred orientation. The addition of

glue, although further decreasing the CE, resulted in a typical glue-type morphology (Fig. 7(d)) (3) and a preferred [101] orientation (Table 1).

The presence of In in the electrolyte had no effect on the CE, and as expected, the deposit morphology (Fig. 7(b)) and preferred orientation (Table 1) were similar to those obtained for deposits electrowon from addition-free electrolyte (3). The addition of glue (Fig. 7(e)) did not significantly change the deposit morphology but did alter the preferred orientation from [112] to [114][101] (Table 1).

The presence of Tl in the electrolyte produced a significant change in the zinc deposit morphology (Fig. 7(c)). The deposit morphology consisted of large hexagonal platelets with serrated edges, similar to that obtained from electrolyte containing <5 mg/L Pb (12). The preferred deposit orientation was [101] (Table 1) and this was also similar to that obtained for deposits electrowon from Pb-contaminated electrolytes (12). The addition of glue further enhanced this morphology type (Fig. 7(f)), but the zinc platelets became vertically aligned to the Al cathode resulting in a preferred [100][110][112] orientation (Table 1).

The effect of the Group VA impurities (As, Bi) on the morphology of the 1-h zinc deposits electrowon at 430 A/m^2 in the presence and absence of glue is shown in a series of SEM photomicrographs, Figure 8. The preferred deposit orientations of selected deposits electrowon in the presence of these impurities, with and without glue, are summarized in Table 2.

As indicated by Figure 8(a), the presence of 40 mg/L As(III) in the electrolyte had no effect on the morphology of the 1-h zinc deposit which was identical to that electrowon from addition-free electrolyte. Similarly, the deposit orientation (Table 2) remained unchanged. The presence of glue resulted in a typical glue-type deposit morphology (Fig. 8(d)) and [101] preferred orientation, Table 2.

Increasing As(V) concentrations in the electrolyte resulted in a change in preferred orientation according to the sequence, [112] → [114] → [002], Table 2. The deposit morphology obtained for 10 mg/L As(V) is shown in Figure 8(b) and is seen to consist of flat, circular platelets oriented at low angles to the Al cathode. The addition of 10 mg/L glue changed the deposit orientation to [101] (Table 2) and the morphology to glue-type, Figure 8(d).

The deposit morphology obtained in the presence of Bi, Figure 3(c), consisted of poorly defined, irregularly-shaped crystals indicative of deposit re-solution. The addition of glue, Figure 8(f), refined the deposit grain size but otherwise did not improve the morphology; the preferred orientation remained [002], Table 2, even in the presence of added glue.

The effect of the Group VIA impurities (Se, Te) on the morphology and orientation of the 1-h Zn deposits electrowon at 430 A/m^2 in the presence and absence of glue is shown in Figure 9 and Table 3, respectively. The presence of Se in the electrolyte resulted in a Zn deposit morphology consisting of large, flat clusters, Figure 9(a), having a preferred [002] orientation, Table 3. This deposit morphology was very similar to that obtained when the electrolyte contained Sb (3). The addition of glue was not effective in counteracting the effect of Se on the morphology (Fig. 9(c)) or on the preferred orientation, Table 3.

The deposit morphology realized in the presence of Te, Figure 9(b), was similar to that obtained when the electrolyte contained Bi (cf. Fig. 8(c)). The preferred orientation was [105], Table 3, indicating that the zinc crystals were aligned at low angles to the Al cathode. The addition of glue did not improve the deposit morphology, Figure 9(d), but did change the preferred orientation to [101][100], Table 3.

3.3 Polarization Effects

The typical cyclic voltammogram obtained for addition-free, purified industrial acid sulphate electrolyte is shown in Figure 10. A cycle starting from point A (-0.95 V vs SCE) goes through a region of low current until point B where zinc deposition commences. The current increases to point C where the scan is reversed. The current then decreases, reaches zero at point D where it becomes anodic corresponding to the dissolution of deposited zinc. The anodic peak is reached at E and dissolution is complete on return to A.

The region BCD is called a nucleation hysteresis loop and is characterized by several important features. The current for the initial deposition of zinc (point B) does not become appreciable until well beyond the zinc reversible potential. The point B has been used to define a "nucleation overpotential" B-D. However, the position of B can be defined only loosely as it appears to shift with the sensitivity at which the current is recorded and with the sweep rate. The position of B also shifts when certain impurities and/or organics are added to the electrolyte. For example, relative to the addition-free electrolyte, the point B occurs at a less negative potential when Sb is present in the electrolyte but becomes more negative for glue-containing electrolytes (2,3).

The current on the descending branch of the loop (CD) is higher than on the ascending branch because, at a given potential, there are more and larger zinc nuclei available while the charge-transfer rate constant is the same. The cathodic overpotential in this region is associated essentially with zinc deposition onto freshly deposited zinc and has been termed "plating overpotential". The plating overpotential has been found to be sensitive to the presence of certain organic additives in both lead and copper electrorefining (18).

The descending branch crosses the zero current axis at point D, the crossover potential (2), at or close to the reversible potential of the system.

The presence of In in the electrolyte had no effect on the cyclic voltammogram for zinc which was identical to that shown in Figure 10 for the addition-free electrolyte. This is in agreement with both the deposit morphology and orientation results which are also similar to the results obtained for the addition-free electrolyte. Data presented in Table 4 indicate that In was not detected in the zinc deposits.

The effect of 15 mg/L Ga on the cyclic voltammogram for zinc is shown in Figure 11 together with the curve for the addition-free electrolyte. It can be seen that the presence of Ga in the electrolyte has a pronounced effect on zinc deposition polarization. The cyclic voltammogram is characterized by a significant cathodic current prior to the zinc decomposition potential. More significant is the fact that in the presence of Ga, the zinc decomposition potential occurs at a more positive potential value than it does for the addition-free electrolyte. This indicates that Ga has a strong depolarizing effect on zinc deposition, in agreement with the low CE obtained under these experimental conditions. The preferred orientation, however, remains {112} similar to the addition-free deposit, and this is unusual when the reaction is depolarized.

The reverse scan in the presence of Ga is characterized by a small plateau region prior to the crossover potential and by a very much reduced anodic dissolution peak. This indicates that zinc re-solution is occurring prior to the crossover potential while the current is still cathodic, suggesting that localized Zn-Ga cells may be responsible. Further, the shift in the crossover potential to more positive values in the presence of

Ga may indicate Zn-Ga alloy formation. Data in Table 4 indicate that Ga does co-deposit with zinc. Similar effects were noted earlier for electrolytes containing Ge (7,11) or Sn (19).

The effect of 10 mg/L Tl on the cyclic voltammogram for zinc is compared to the addition-free curve in Figure 12. Thallium also has a significant effect on zinc deposition polarization, but the effect is different from that of Ga, cf. Figure 11. Thallium shifts the zinc decomposition potential to a more negative value, hence increasing polarization. This results in a preferred [101] deposit orientation (Table 1). The presence of Tl also causes a significant increase in the plating overpotential (Figure 12); also, the current does not return to zero immediately after the anodic dissolution peak, but remains anodic at the end of the scan. Thallium co-deposited with zinc to a significant degree (Table 4) and this may account for its strong influence on the zinc deposit orientation and zinc deposition polarization.

The effects of As(III) and As(V) on the cyclic voltammogram for zinc deposition are compared to the addition-free case in Figure 13. For 50 mg/L As(III), there is a significant cathodic current prior to the zinc decomposition potential; however, the remainder of the voltammogram is very similar to the addition-free case, except that following anodic dissolution of zinc, the current becomes cathodic again.

The initial stage of the As(V) curve is similar to that of As(III). Pentavalent arsenic, however has a significant depolarizing effect on zinc deposition. Also the reverse scan is characterized by plateau region and there is no anodic current. This result is similar to that obtained for Ge (7,11) where it was found that zinc re-solution occurred while the current was still cathodic. This effect was attributed to localized Zn-Ge corrosion cells. The cyclic voltammogram for As(V) is similar to that for Ga (Fig. 11) except that

the BCD hysterisis loop for As(V) is more pronounced than that for Ga, and the curve for Ga has a small anodic current.

The effect of Bi on zinc deposition polarization is shown in the cyclic voltammogram, Figure 14. It can be seen that this curve is almost identical to that obtained for Ga (cf. Fig. 11), except there is no cathodic current prior to Zn deposition or after Zn dissolution. The effect of glue in combination with Bi on zinc deposition polarization is also shown in Figure 14. Although glue increases both the nucleation and plating overpotentials, it also increases the plateau region prior to the crossover potential. Thus, glue is not effective in counteracting the adverse effect of Bi. This is in agreement with the CE (Figure 4) and deposit orientation results, Table 2. Significant quantities of Bi also co-deposited with Zn (Table 4) and this may be a factor in its strong influence on deposit orientation and zinc deposition polarization.

The effects of Se and Te on zinc deposition polarization are shown in Figures 15 and 16, respectively. Both these impurities strongly depolarized the zinc deposition reaction, and the initial ABC portion of the voltammograms are very similar to that obtained for Sb (3) which is also a strong depolarizer. The reverse scan of both curves (Figure 15 and 16), unlike that for Sb (3), was charcterized by plateau regions and small anodic dissolution peaks. The effect of glue with Se, Figure 15, was similar to that observed with Bi (cf., Fig. 14).

4. CONCLUSIONS

The effects of As(III), As(V), Bi, Ga, In, Se, Te and Tl and their interactions with glue on the current efficiency and polarization behaviour of zinc deposition and on the morphology and orientation of 1-h zinc deposits electrowon from industrial acid sulphate electrolyte have been determined.

In and As(III) had no significant effect on the CE or on the deposit morphology and orientation. The cyclic voltammograms obtained in the presence of In and As(III) were very similar to that obtained from addition-free electrolyte; however, the presence of As(III) in the electrolyte results in a significant current prior to the zinc deposition hysteresis loop, BCD, portion of the voltammogram.

Gallium and Bi caused a significant and similar decrease in CE, but the deposit orientation was [002] for Bi-containing electrolyte whereas the deposit orientation obtained in the presence of Ga was similar to that for addition-free electrolyte; i.e., [112]. The deposit morphology obtained in the presence of Bi consisted of irregularly shaped crystals whereas that for Ga was similar to the addition-free morphology in agreement with the [112] orientation. This difference may be related to the fact that Bi co-deposits with zinc to a much greater extent than does Ga (Table 4).

The cyclic voltammograms obtained from electrolytes containing Bi or Ga were very similar to one another, but were quite different from the addition-free voltammogram. Both Bi and Ga depolarize zinc deposition and a shoulder appears on the reverse scan portion of the curve, indicative of zinc resolution.

In some respects, As(V) is similar to Ga and Bi in its effect on zinc deposition polarization. The BCD hysteresis loop is similar in shape, but is much larger in the case of As(V); As(V) causes a significant cathodic current prior to the zinc deposition hysteresis loop and after the anodic dissolution of zinc. In this respect, As(V) is similar to As(III). Pentavalent arsenic causes a dramatic decrease in the CE for zinc deposition, that is greater than for Bi or Ga. The effect of As(V) on the preferred orientation of the zinc deposits depends on its concentration in the electrolyte. The preferred

orientation changes from {112} → {002} → {101} with increasing As(V) concentration. The deposit morphology obtained from an electrolyte containing 10 mg/L As(V) was characterized by poorly-defined hexagonal platelets aligned at low angles to the Al cathode.

The presence of Tl in the electrolyte increased zinc deposition polarization resulting in [101] → [110] → [100] preferred orientations and an increase in current efficiency. The resulting triangular-type morphology was similar to that obtained from electrolytes containing Pb. Thallium also co-deposited with zinc to a greater extent than any of the other impurities.

Both Se and Te depolarized zinc deposition and the voltammograms were characterized by a shoulder on the reverse scan portion of the curve. The deposit orientations were [002] and [$\bar{1}$05], respectively, and the morphology consisted of large, non-distinct clusters of poorly defined crystals.

In general, glue was not effective in counteracting the detrimental behaviour of these impurities in zinc electrowinning.

ACKNOWLEDGEMENTS

Thanks are due to Cominco Ltd. for providing the electrolyte. D. Owens, CANMET, did the scanning electron microscopy on the zinc deposits and P. Carriere, CANMET, carried out the X-ray diffraction analyses.

REFERENCES

1. Robinson, D.J. and O'Keefe, T.J. "On the effects of antimony and glue on zinc electrocrystallization behavior"; J Appl Electrochem 6:1-7; 1976.

2. Lamping, B.A. and O'Keefe, T.J. "Evaluation of zinc sulphate electrolyses by cyclic voltammetry and electron microscopy"; Metall Trans 7B:551-558; 1976.

3. MacKinnon, D.J. and Brannen, J.M. "Zinc deposit structures obtained from high purity synthetic and industrial acid sulphate electrolytes with and without antimony and glue additions"; J Appl Electrochem 7:451-459; 1977.

4. Maja, M. and Spinelli, P. "Detection of metallic impurities in acid zinc plating baths"; J Electrochem Soc 118:1538-1540; 1971.

5. Wark, I.W. "The electrodeposition of zinc from acidified zinc sulphate solution"; J Appl Electrochem 9:721-730; 1979.

6. Maja, M., Spinelli, P., Fratesi, R. and Roventi, G. "Zinc electrocrystallization from impurity-containing sulphate baths"; J Electrochem Soc 129:2695-2700; 1982.

7. Fosnacht, D.R. and O'Keefe, T.J. "Evaluation of zinc sulphate electrolytes containing certain impurities and additives by cyclic voltammetry"; J Appl Electrochem 10:495-504; 1980.

8. Fratesi, R., Roventi, G., Maja, M. and Penazzi, N. "Effects of nickel impurities on zinc electrodeposition"; J Appl Electrochem 10:765-774; 1980.

9. Wang, Yar-Ming, O'Keefe, T.J. and James, W.J. "Voltammetric evaluation of zinc electrowinning solution containing nickel"; J Electrochem Soc 127:2589-2593; 1980.

10. MacKinnon, D.J., Morrison, R.M. and Brannen, J.M. "The effects of nickel and cobalt and their interaction with antimony on zinc electrowinning from industrial acid sulphate electrolyte"; J Appl Electrochem in press.

11. MacKinnon, D.J. and Fenn, P.L. "The effect of germanium on zinc electrowinning from industrial acid sulphate electrolyte"; J Appl Electrochem 14:467-474; 1984.

12. MacKinnon, D.J., Brannen, J.M. and Kerby, R.C. "The effect of lead on zinc deposit structures obtained from high purity synthetic and industrial acid sulphate electrolyte"; J Appl Electrochem 9:55-70; 1979.

13. MacKinnon, D.J., Brannen, J.M. and Kerby, R.C. "The effect of cadmium on zinc deposit structures obtained from high purity industrial acid sulphate electrolyte"; J Appl Electrochem 9:71-79; 1979.

14. Foulkes, F.R., Smith, J.W., Kalia, R. and Kirk, D.W. "Effects of cadmium impurities on the electrowinning of zinc"; J Electrochem Soc 128:2307-2314; 1981.

15. Weaver, G.T. "Effect of control of impurities in the electrowinning of zinc"; J of Metals 11:130-134; 1959.

16. Kerby, R.C. and Ingraham, T.R. "Effect of impurities on the current efficiency of zinc electrodeposits"; Mines Branch, Energy, Mines and Resources Canada; Res. Rept. R243; 1971.

17. Kirk-Othner, Encyclopedia of Chemical Technology, 2nd Ed. 22:588.

18. Andersen, T.N., Kerby, R.C. and O'Keefe, T.J. "Control techniques for industrial electrodeposition from aqueous solutions"; J of Metals 37:36-43; 1985.

19. MacKinnon, D.J. and Fenn, P.L. "The effect of tin on zinc electrowinning from industrial acid sulphate electrolyte"; J Appl Electrochem 14:701-707; 1984.

Table 1. The Effect of Gallium, Indium and Thallium With and Without Glue on the Preferred Orientation of Zinc Deposits Electrowon from Industrial Acid Sulphate Electrolyte

Ga (mg/L)	In (mg/L)	Tl (mg/L)	Glue (mg/L)	Orientation[1]
0	0	0	0	[112] [114] [102]
5	0	0	0	[112] [102]
20	0	0	0	[112]
20	0	0	10	[112]
20	0	0	50	[101]
0	20	0	0	[112] [103]
0	20	0	20	[114] [101]
0	0	20	0	[101]
0	0	20	10	[100] [110] [112]

[1] Relative to ASTM standard for zinc powder. Electrolysis conditions: 55 g/L Zn; 150 g/L H_2SO_4; 35°C; 430 A/m^2.

Table 2. The Effect of Arsenic and Bismuth With and Without Glue on the Preferred Orientation of Zinc Deposits Electrowon from Industrial Acid Sulphate Electrolyte

As(III) (mg/L)	As(V) (mg/L)	Bi (mg/L)	Glue (mg/L)	Orientation[1]
0	0	0	0	[112] [114] [102]
5	0	0	0	[101]
10	0	0	0	[112] [101]
50	0	0	0	[112]
40	0	0	5	[101]
40	0	0	20	[101]
0	5	0	0	[112] [110]
0	10	0	0	[114] [112]
0	20	0	0	[002] [105]
0	10	0	5	[112]
0	10	0	10	[101]
0	10	0	30	[101]
0	0	10	0	[002]
0	0	20	0	[002]
0	0	20	5	[002]
0	0	20	10	[002]
0	0	20	20	[002]
0	0	20	50	[002]

[1] Relative to ASTM standard for zinc powder. Electrolysis conditions: 55 g/L Zn; 150 g/L H_2SO_4; 35°C; 430 A/m^2.

Table 3. The Effect of Selenium and Tellurium With and Without Glue on the Preferred Orientation for Zinc Deposits Electrowon from Industrial Acid Sulphate Electrolyte

Se (mg/L)	Te (mg/L)	Glue (mg/L)	Orientation[1]
0	0	0	[112] [114] [102]
2	0	0	[002]
2	0	10	[002]
0	2	0	[105]
0	2	10	[101] [100]

[1] Relative to ASTM standard for zinc powder. Electrolysis conditions: 55 g/L Zn; 150 g/L H_2SO_4; 35°C; 430 A/m^2.

Table 4. Co-deposition of Various Impurities with Zinc

Impurity	Concentration in solution (mg/L)	Glue (mg/L)	Concentration in Zn deposit (ppm)
Ga	50	0	<80
Ga	20	50	<50
In	50	0	n.d.
In	20	50	n.d.
Tl	50	0	5700
Tl	20	50	3300
As(III)	50	0	10
As(III)	40	30	10
As(V)	10	30	<6
Bi	30	0	2100
Bi	20	50	1100

n.d. = not detected

Electrolysis conditions: 55 g/L Zn; 150 g/L H_2SO_4; 35°C; 430 A/m^2

FIGURE CAPTIONS

Figure 1. Plots showing the effects of increasing concentrations of Ga, In and Tl on the current efficiency for 1-h Zn deposits electrowon at 430 A/m^2 from industrial acid sulphate electrolyte.

Figure 2. Plots showing the effect of increasing glue concentrations in combination with a fixed concentration of Ga, In and Tl on the current efficiency for 1-h Zn deposits electrowon at 430 A/m^2 from industrial acid sulphate electrolyte.

Figure 3. Plots showing the effects of increasing concentrations of As(III), As(V) and Bi on the current efficiency for 1-h Zn deposits electrowon at 430 A/m^2 from industrial acid sulphate electrolyte.

Figure 4. Plots showing the effect of increasing glue concentrations in combination with a fixed concentration of As(III), As(V) and Bi on the current efficiency for 1-h Zn deposits electrowon at 430 A/m^2 from industrial acid sulphate electrolyte.

Figure 5. Plots showing the effects of increasing concentrations of Se and Te on the current efficiency for 1 h Zn deposits electrowon at 430 A/m^2 from industrial acid sulphate electrolyte.

Figure 6. Plots showing the effect of increasing glue concentrations in combination with a fixed concentration of Se and Te on the current efficiency for 1-h Zn deposits electrowon at 430 A/m^2 from industrial acid sulphate electrolyte.

Figure 7. SEM photomicrographs showing the effect of Ga, In and Tl with and without glue on the morphology of 1-h Zn deposits electrowon at 430 A/m^2 from industrial acid sulphate electrolyte.

Figure 8. SEM photomicrographs showing the effect of As(III), As(V) and Bi with and without glue on the morphology of 1-h Zn deposits electrowon at 430 A/m^2 from industrial acid sulphate electrolyte.

Figure 9. SEM photomicrographs showing the effect of Se and Te with and without glue on the morphology of 1-h Zn deposits electrowon at 430 A/m^2 from industrial acid sulphate electrolyte.

Figure 10. Cyclic voltammogram obtained for addition-free industrial acid zinc sulphate electrolyte.

Figure 11. Cyclic voltammograms showing the effect of Ga on zinc deposition polarization.

Figure 12. Cyclic voltammograms showing the effect of Tl on zinc deposition polarization.

Figure 13. Cyclic voltammograms showing the effects of As(III) and As(V) on zinc deposition polarization.

Figure 14. Cyclic voltammograms showing the effects of Bi and Bi + glue on zinc deposition polarization.

Figure 15. Cyclic voltammograms showing the effects of Se and Se + glue on zinc deposition polarization.

Figure 16. Cyclic voltammograms showing the effect of Te on zinc deposition polarization.

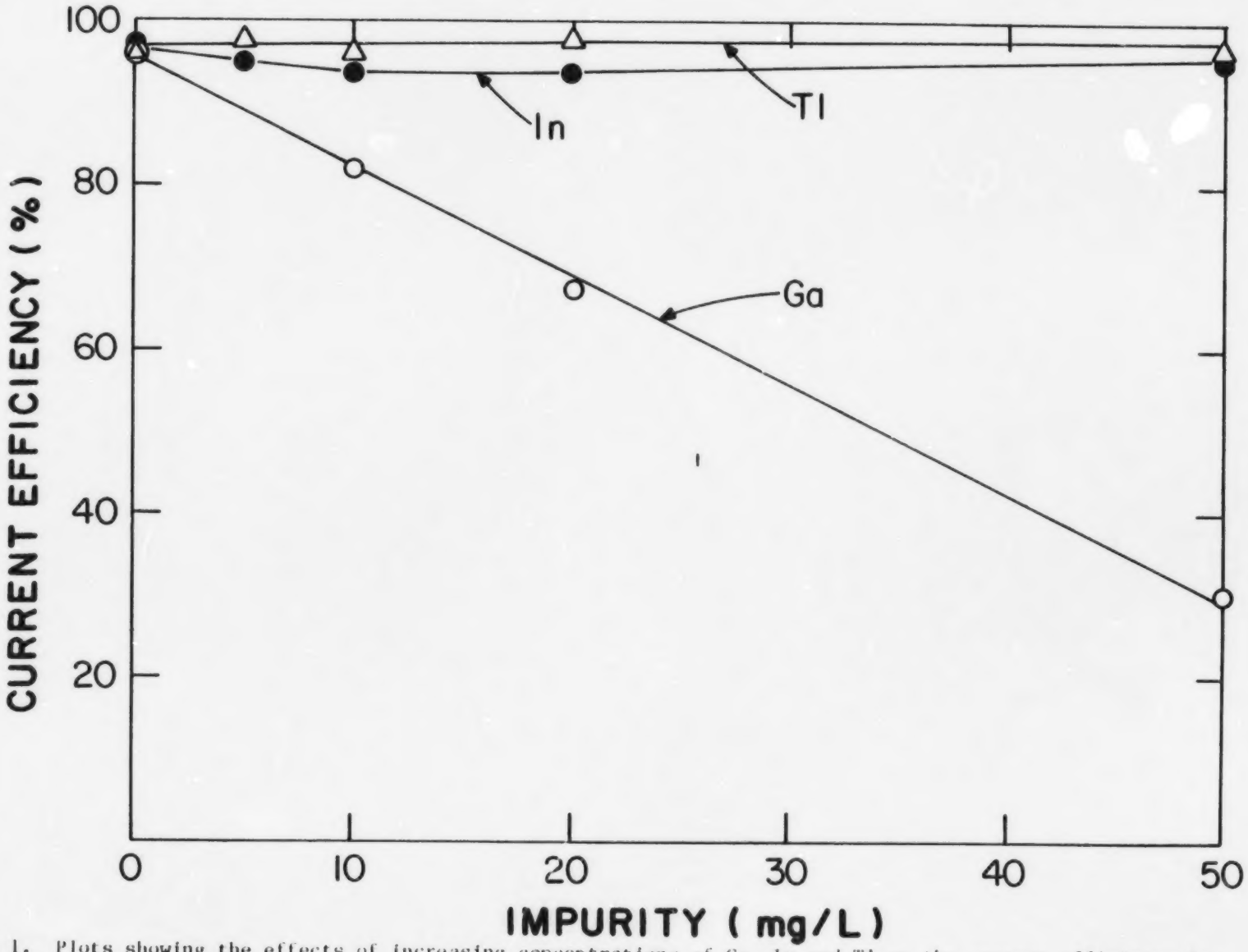

Fig. 1. Plots showing the effects of increasing concentrations of Ga, In and Tl on the current efficiency for 4-4 Zn deposits electrowon at 430 A/m^2 from industrial acid sulphate electrolyte.

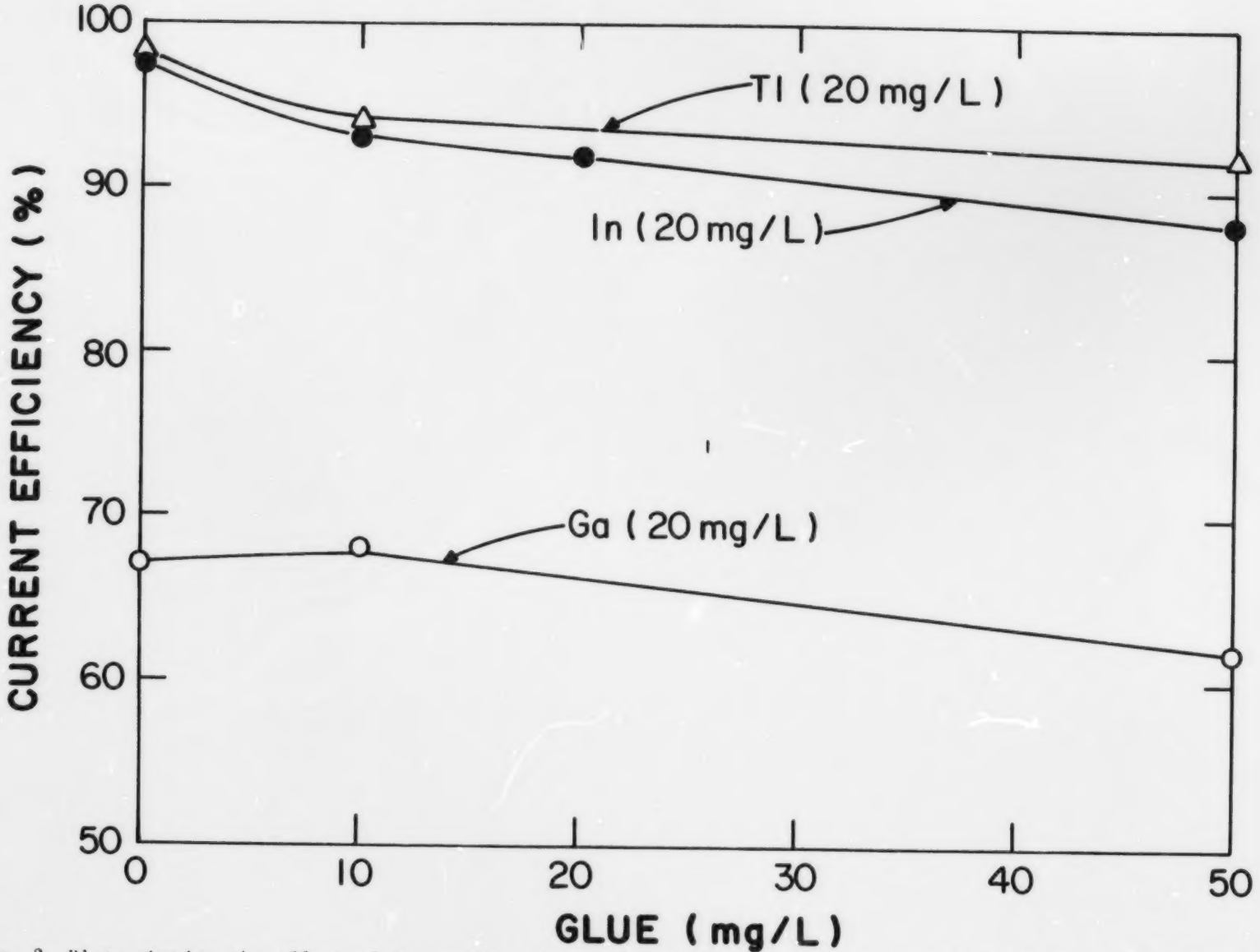

Fig. 2 Plots showing the effect of increasing glue concentrations in combination with a fixed concentration of Ga, In and Tl on the current efficiency for 1-h Zn deposits electrowon at 430 A/m^2

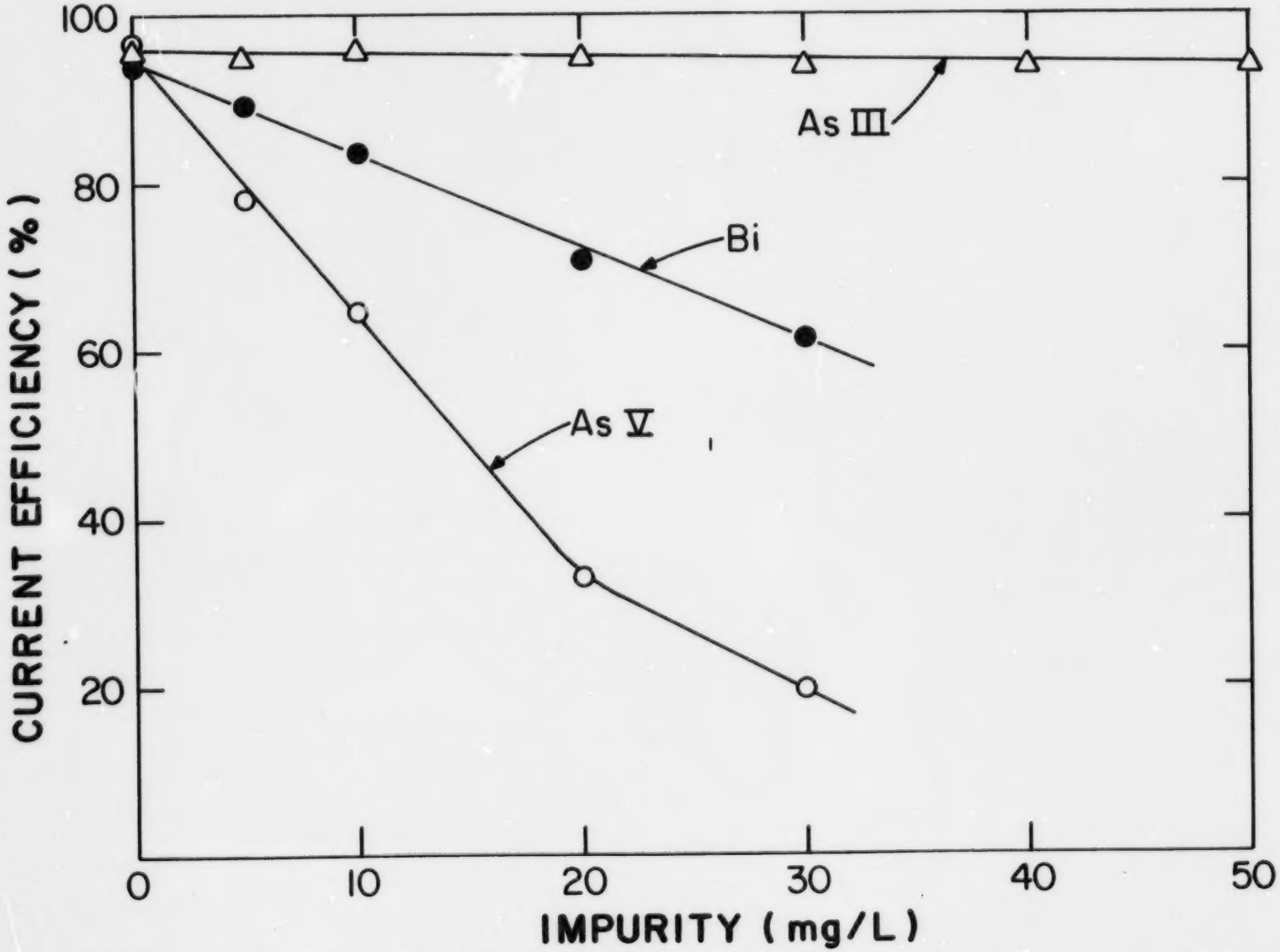

Fig. 3. Plots showing the effects of increasing concentrations of As(III), As(V) and Bi on the current efficiency for 1-h Zn deposits electrowon at 430 A/m^2.

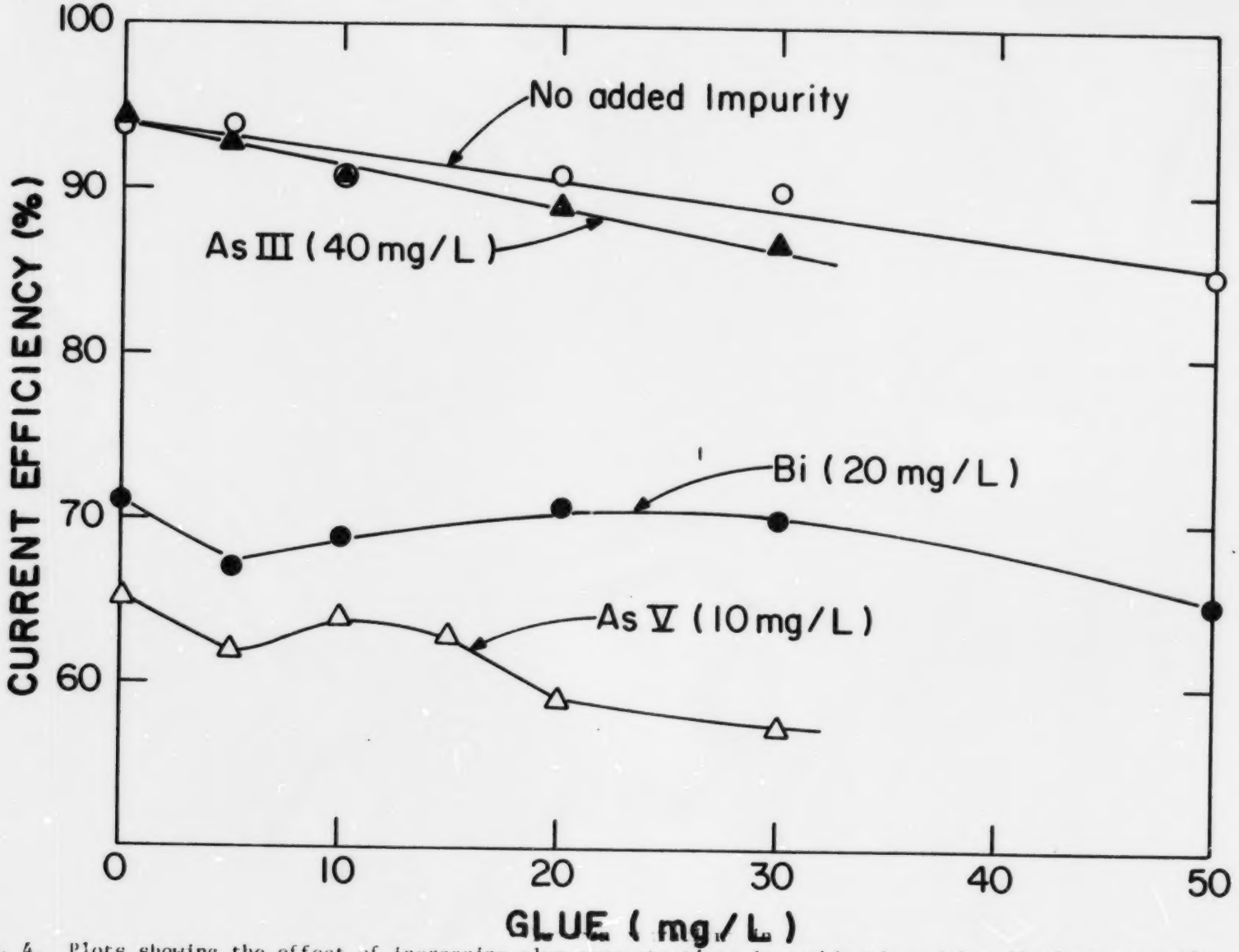

Fig. 4. Plots showing the effect of increasing glue concentrations in combination with a fixed concentration of As(III), As(V) and Bi on the current efficiency for 1-h Zn deposits electrowon at 430 A/m^2.

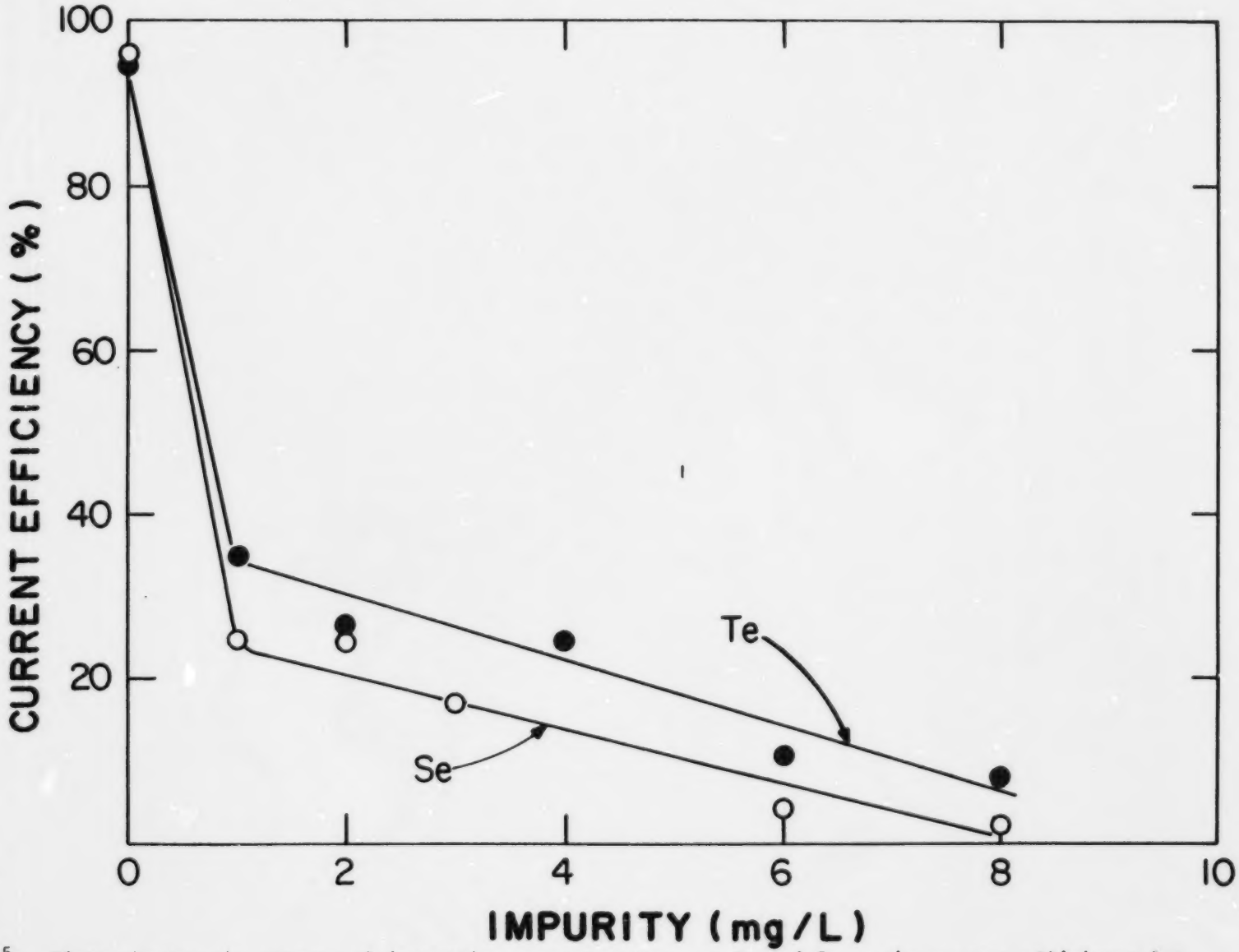

Fig. 5. Plots showing the effects of increasing concentrations of Se and Te on the current efficiency for 1-h Zn deposits electrowon at 430 A/m².

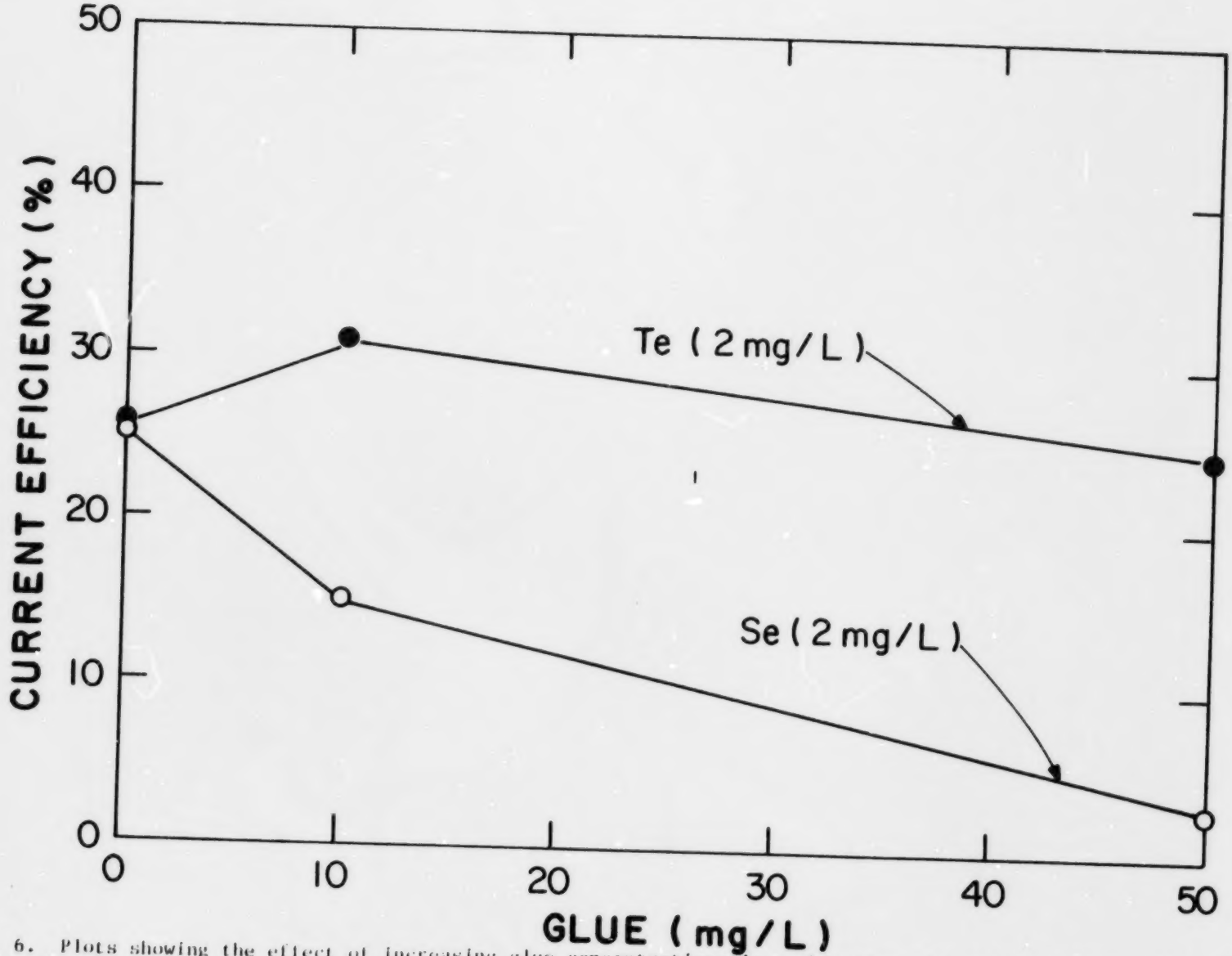

Fig. 6. Plots showing the effect of increasing glue concentrations in combination with a fixed cocentration of Se and Te on the current efficiency for 1-h Zn deposits electrowon at 430 A/m^2.

a) 20 mg/L Ga

b) 20 mg/L In

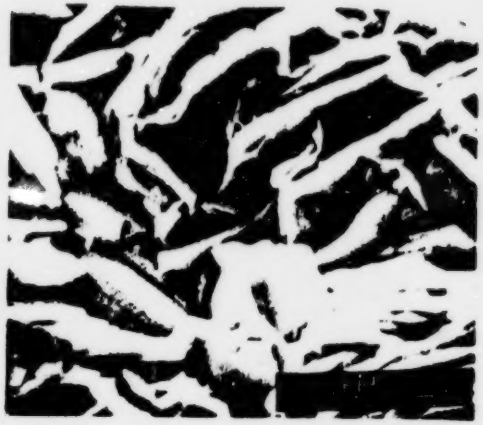

c) 20 mg/L Tl

d) 20 mg/L Ga
50 mg/L Glue

e) 20 mg/L In
20 mg/L Glue

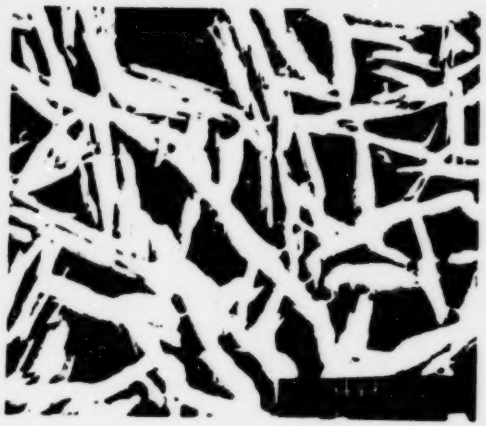

f) 20 mg/L Tl
10 mg/L Glue

Figure 7 - SEM photomicrograph showing the effect of Ga, In and Ti with and without Glue on the morphology of 1-h zinc deposits electrowon at 430 A/m^2.

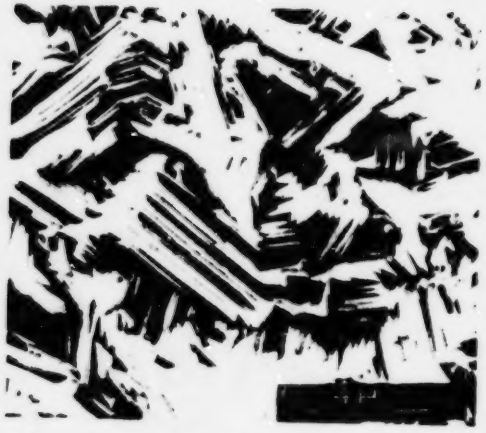

a) 40 mg/L As III

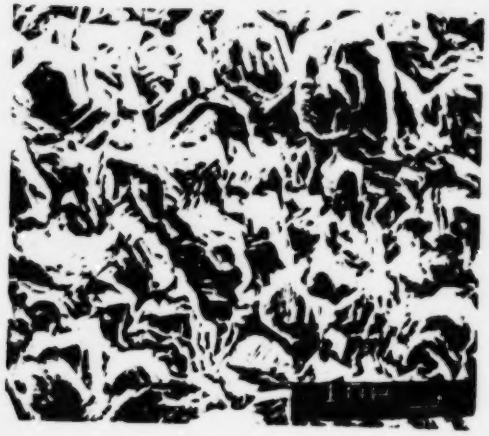

b) 10 mg/L As V

c) 20 mg/L Bi

d) 40 mg/L As III
20 mg/L Glue

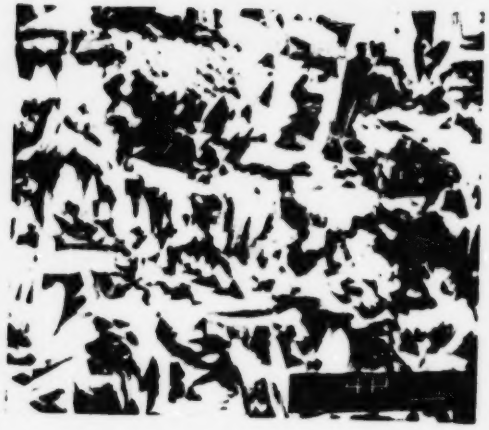

e) 10 mg/L As V
10 mg/L Glue

f) 20 mg/L Bi
10 mg/L Glue

Figure 8 - SEM photomicrographs showing the effect of As and Bi with and without Glue on the morphology of 1-h zinc deposits electrowon at 430 A/m^2.

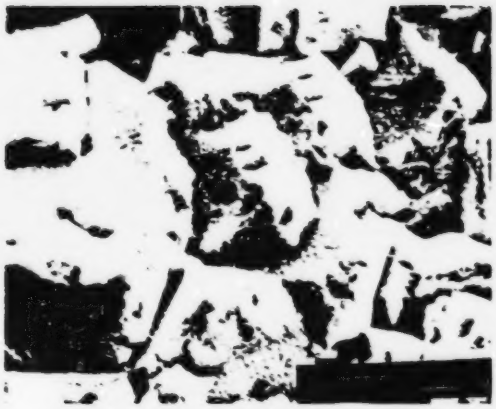

a) 2 mg/L Se

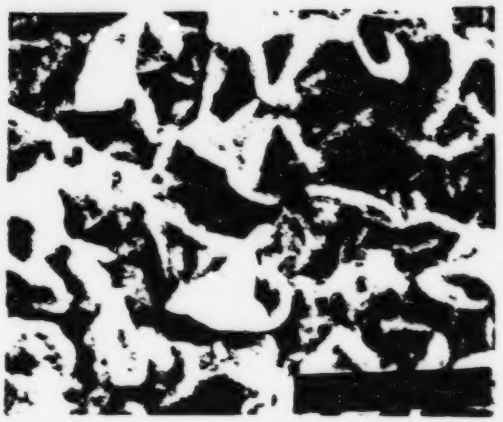

b) 2 mg/L Te

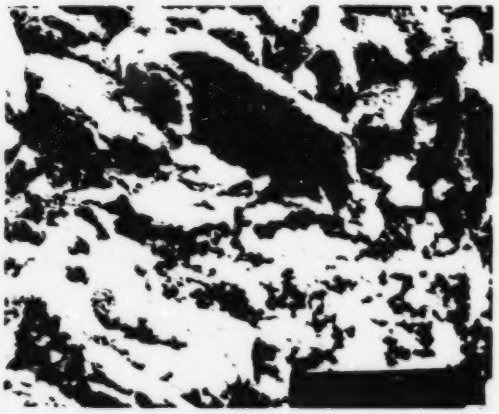

c) 2 mg/L Se
10 mg/L Glue

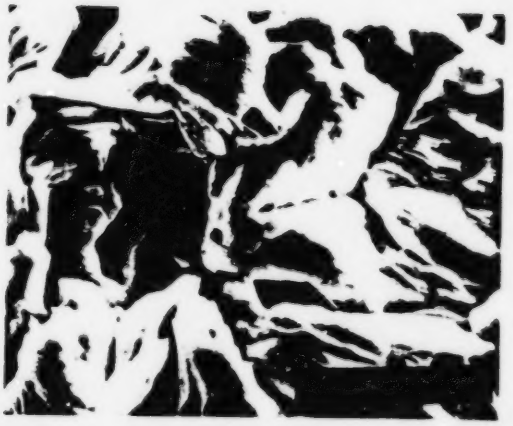

d) 2 mg/L Te
10 mg/L Glue

Figure 9 - SEM photomicrographs showing the effect of Se and Te with and without Glue on the morphology of 1-h zinc deposits electrowon at 430 A/m^2.

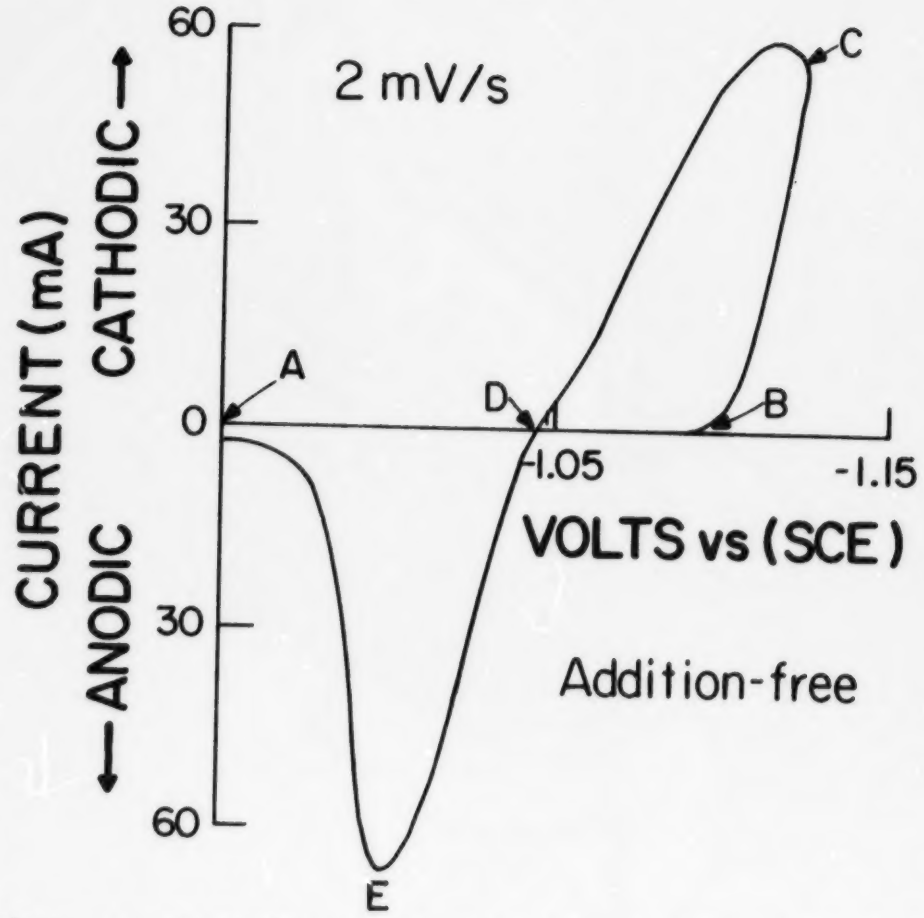

Fig. 10. Cyclic voltammogram obtained for addition-free industrial acid zinc sulphate electrolyte.

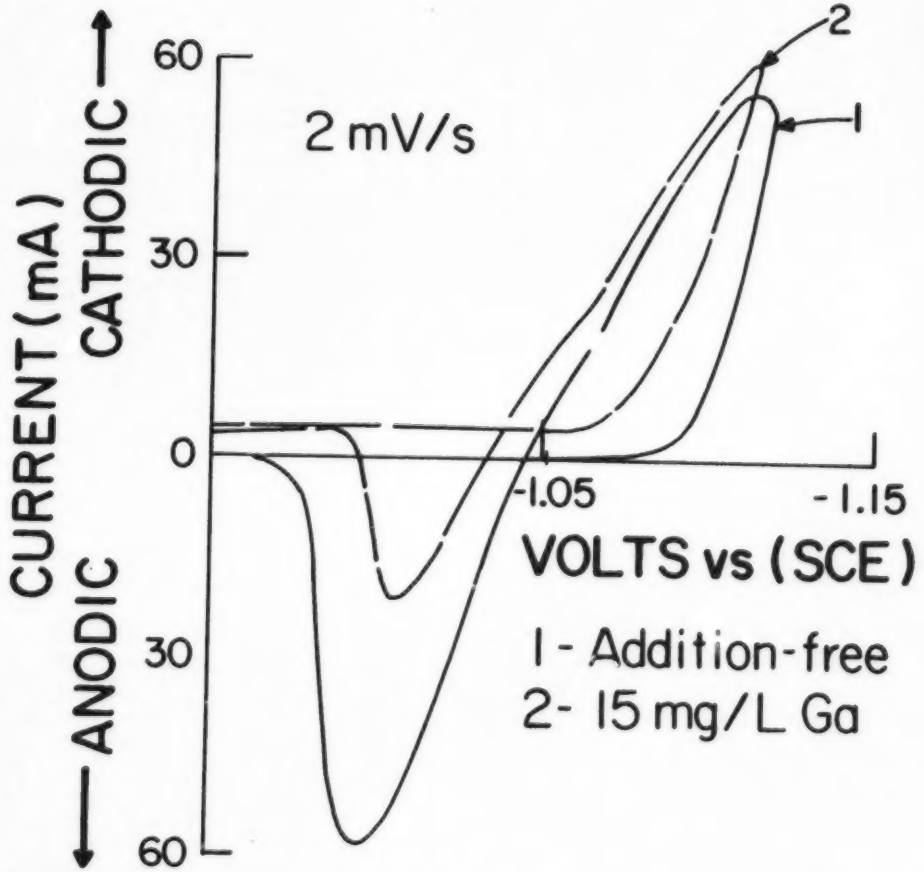

Fig. 11. Cyclic voltammograms showing the effect of Ga on zinc deposition polarization.

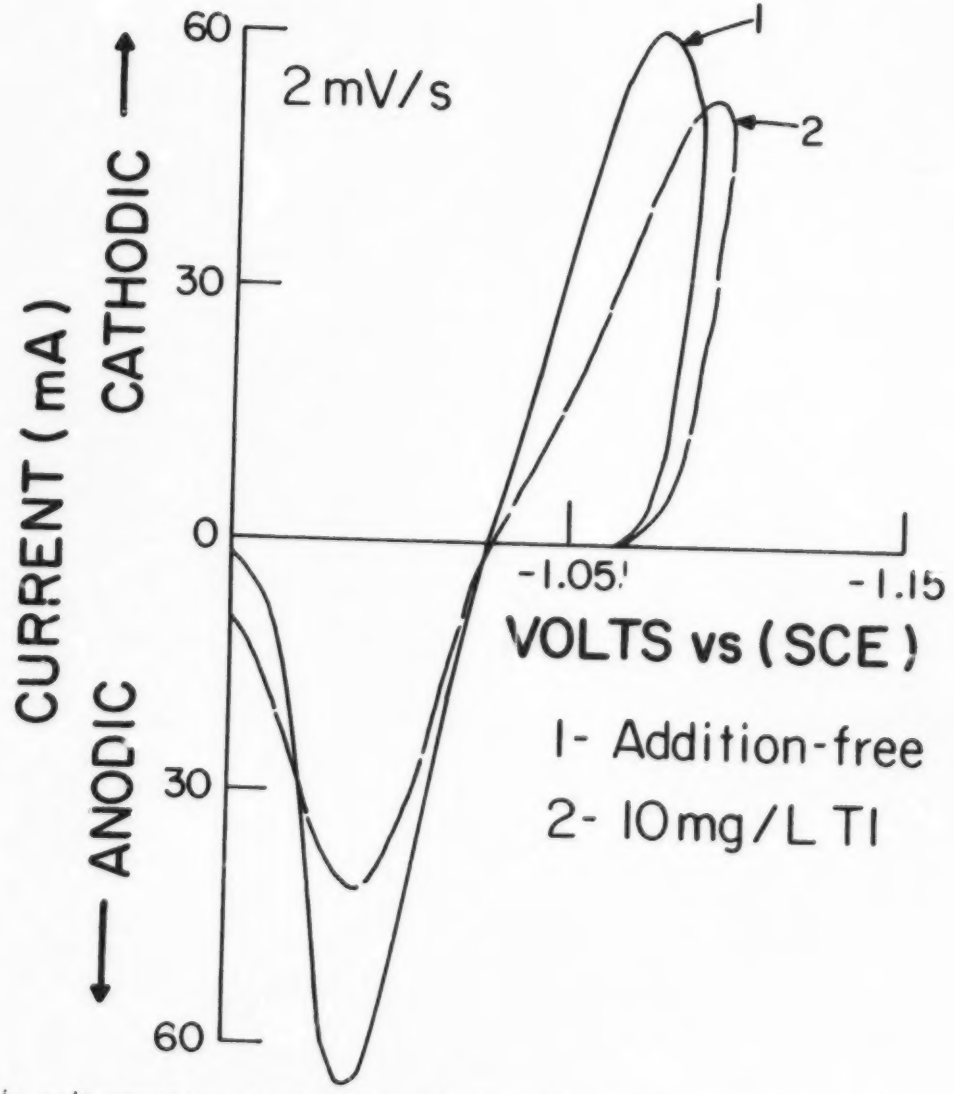

Fig. 12. Cyclic voltammograms showing the effect of Tl on zinc deposition polarization.

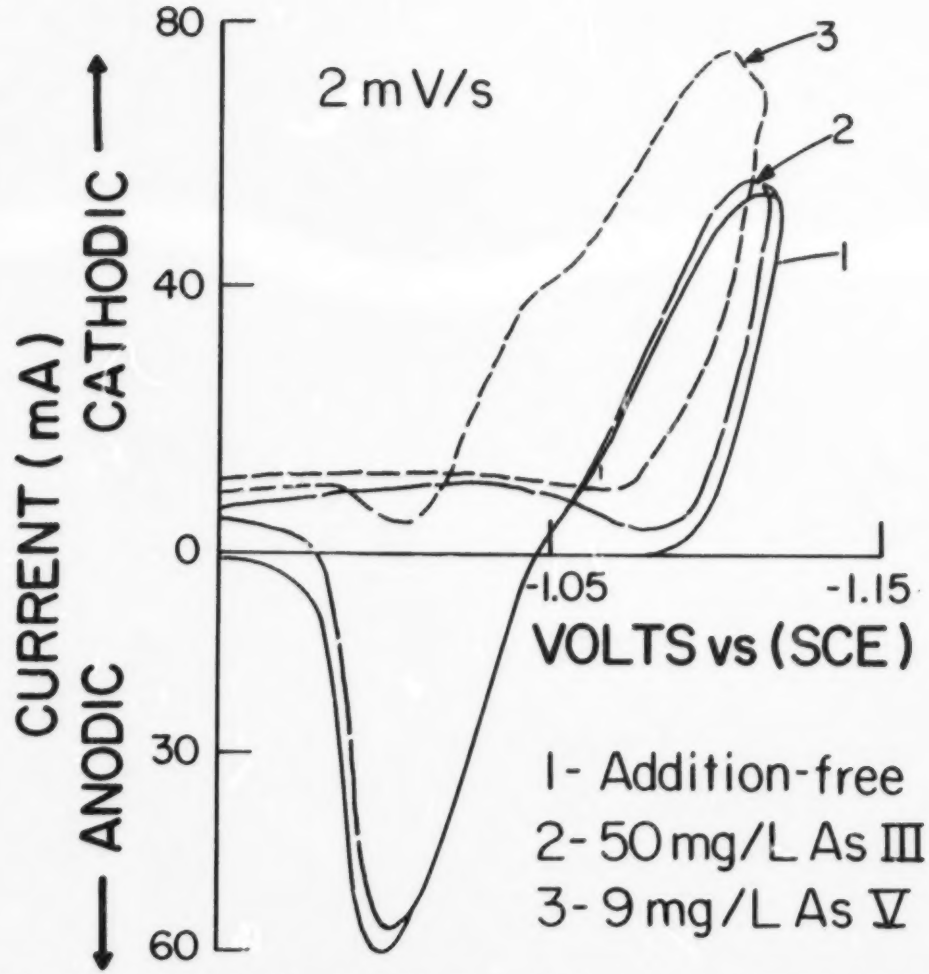

Fig. 13. Cyclic voltammograms showing the effects of As(III) and As(V) on zinc deposition polarization.

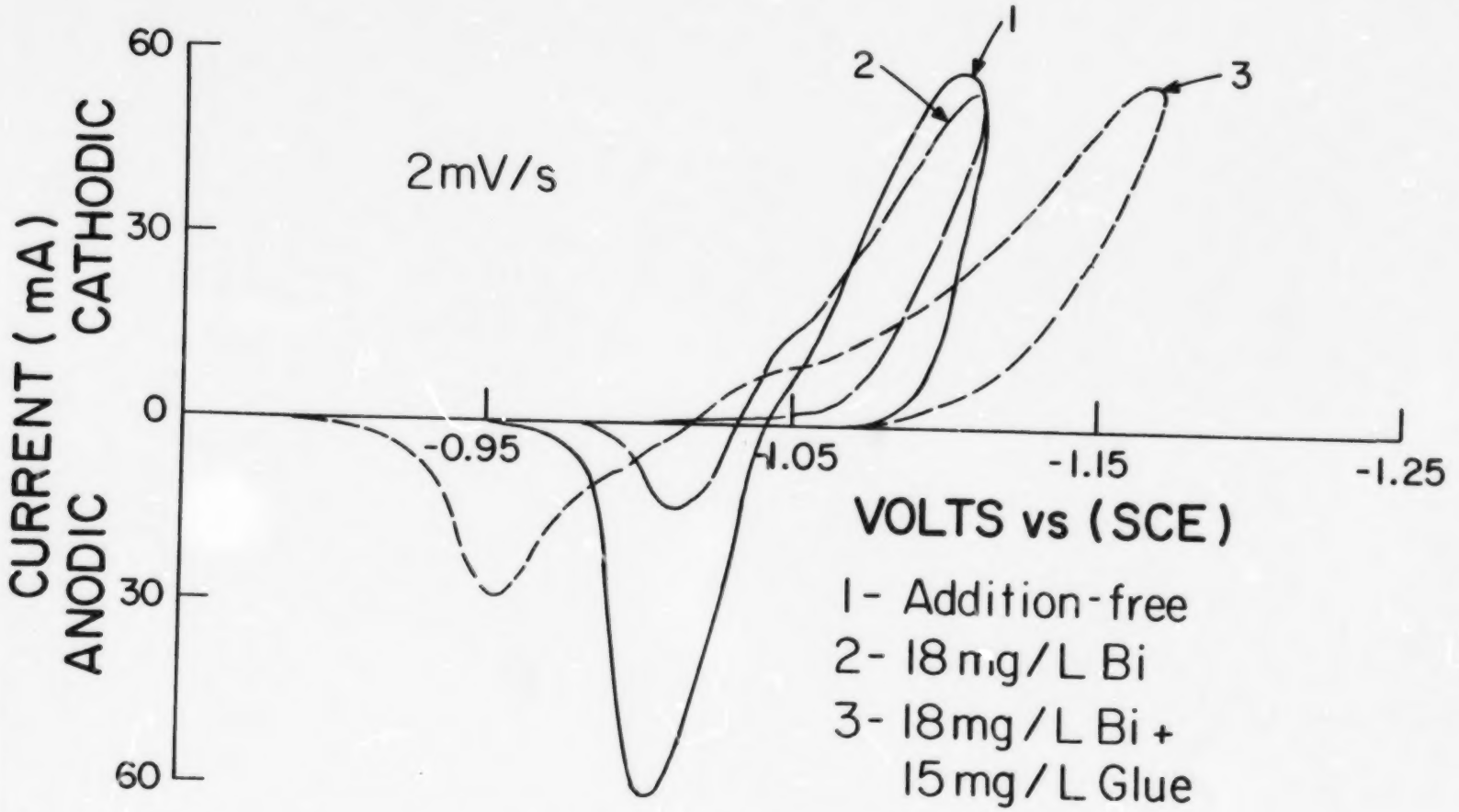

Fig. 14. Cyclic voltammograms showing the effects of Bi and Bi + glue on zinc deposition polarization.

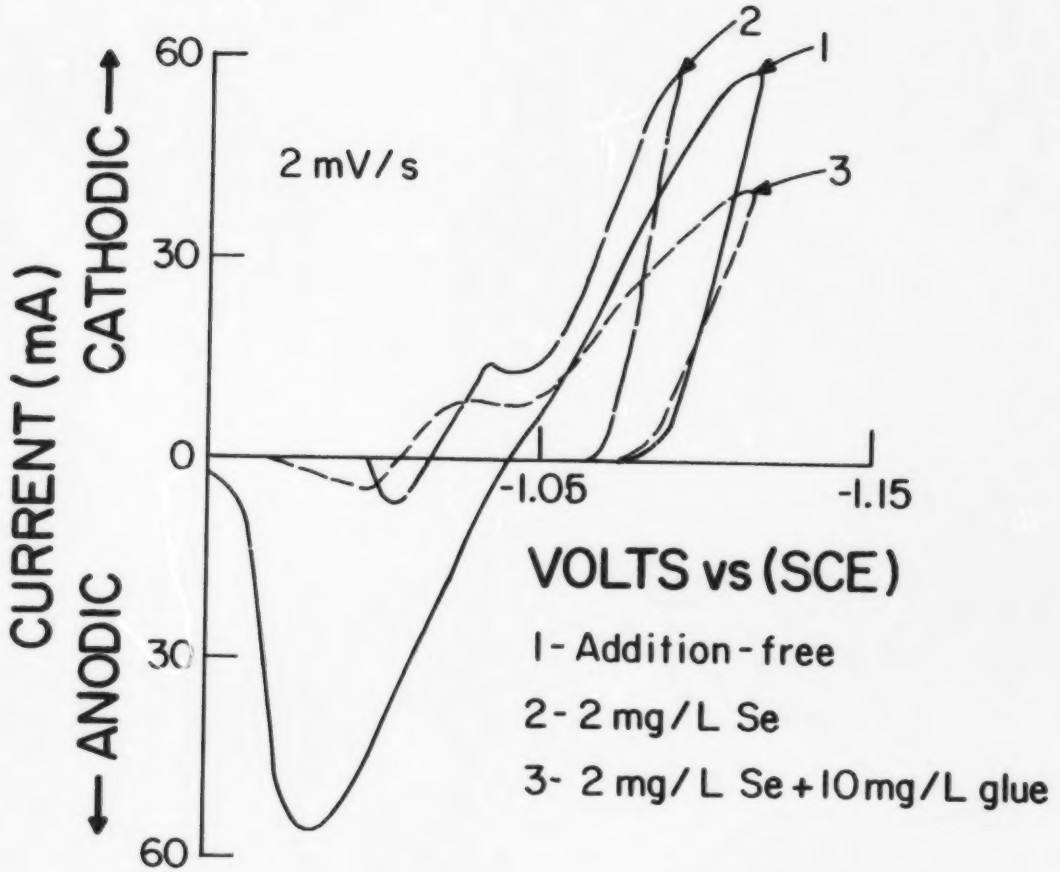

Fig. 15. Cyclic voltammograms showing the effects of Se and Se + glue on zinc deposition polarization.

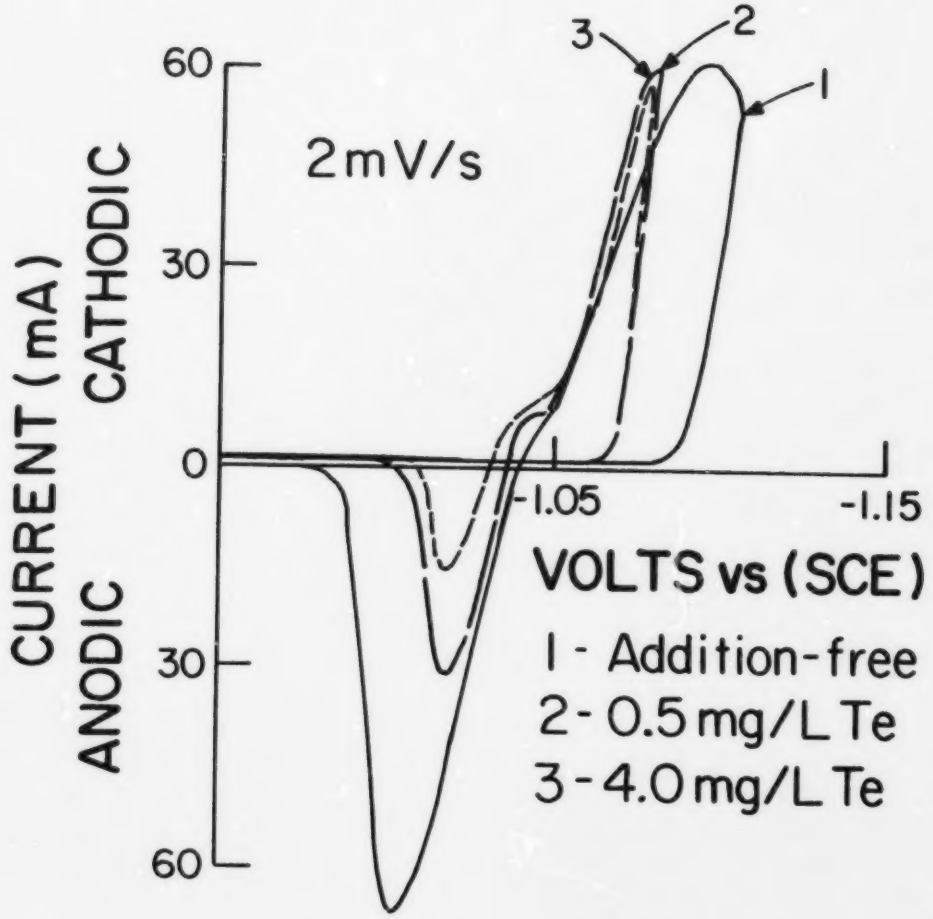

Fig. 16. Cyclic voltammograms showing the effect of Te on zinc deposition polarization.